



2017 ANNUAL MEETING

POSTER SESSIONS

Mon-Wed, March 20-22, 2017 • San Diego Convention Center • San Diego, California

2017 POSTER SESSIONS—SAILS PAVILION

MONDAY–WEDNESDAY

ORS WILL HAVE TWO POSTER SESSIONS

Poster Session 1 (PS1):

Posters will be displayed Monday and Tuesday morning

Poster Session 2 (PS2):

Posters will be displayed Tuesday afternoon and Wednesday

MONDAY, MARCH 20 10:00 AM – 5:30 PM

10:15 AM – 11:15 AM Poster viewing
12:15 PM – 2:15 PM Lunch and Poster Session 1 viewing

Authors at posters to answer questions

EVEN-number poster presenters 1:15 PM – 1:45 PM
ODD-number poster presenters 1:45 PM – 2:15 PM

TUESDAY, MARCH 21

9:00 AM – 11:30 AM; 2:00 PM – 5:00 PM

9:30 AM – 10:30 AM Poster viewing
11:30 AM – 12:00 PM Poster Session 1 Dismantle
1:00 PM – 1:30 PM Poster Session 2 Set-Up
3:45 PM – 4:45 PM Poster viewing

WEDNESDAY, MARCH 22 10:00 AM – 4:00 PM

10:15 AM – 11:15 AM Poster viewing
12:15 PM – 2:15 PM Lunch and Poster Session 2
3:15 PM – 3:45 PM Poster viewing

Authors at posters to answer questions

EVEN-number poster presenters 1:15 PM – 1:45 PM
ODD-number poster presenters 1:45 PM – 2:15 PM

POSTER CATEGORIES	POSTER SESSION 1 #'S	POSTER SESSION 2 #'S
American Academy of Orthopaedic Surgeons (AAOS) Best Posters	AAOS1–AAOS7	AAOS1–AAOS7
Biomaterial	353–420	1310–1379
Board of Specialty Society (BOS) Best Posters	BOS1–BOS10	BOS1–BOS10
Bone	666–780	1627–1744
Cartilage and Synovium	421–514	1380–1473
Diagnostic Imaging	1272–1299	2231–2246
Foot and Ankle	1175–1200	2136–2160
German Society for Orthopaedics and Trauma (DGOU)	Germany	Germany
Guest Nation - China	CHINA1–CHINA3	CHINA1–CHINA3
Hand and Wrist	1156–1174	2117–2135
Hip	966–998	1933–1961
Hip and Knee Arthroplasty	999–1101	1962–2061
Infection and Inflammation	1201–1226	2161–2187
International Combined Orthopaedic Research Society (ICORS) Best Posters	ICORS1–ICORS12	ICORS1–ICORS12
Knee	898–965	1866–1932
Late Breaking Poster Session	2275–2355	2356–2436
Meniscus	515–533	1474–1490
Muscle	642–665	1602–1626
NIRA Finalists	25–33, 43–51, 70–77, 102–109	25–33, 43–51, 70–77, 102–109
Osteoarthritis and forms of Arthropathy	534–585	1491–1540
Poster Teasers	116–160	287–331
Shoulder and Elbow	1102–1155	2062–2116
Spine	781–897	1745–1865
Tendon/Ligament	586–641	1541–1601
Trauma and Fracture	1227–1271	2188–2230
Tumors	1290–1309	2247–2265
Women's Health Issues Board (WHIAB) Best Poster	WHIAB	WHIAB

POSTERS

Poster No. 389

Tuning Alginate Bioinks to Modulate Their Printability and Stiffness in Order to Spatially Direct MSC Fate Within Bioprinted Tissues

Fiona E. Freeman, Daniel J. Kelly

Poster No. 390

Spinal Fusion Using a Novel BioGlass Fiber Combined with Autograft

William R. Walsh, Rema A. Oliver, Chris Christou, Tian Wang, Emma R. Walsh, Vedran Lovric, Matthew H. Pelletier, Shrikar Bondre

Poster No. 391

A Trisulfated Glycosylated Peptide Amphiphile Nanofiber Scaffold for Spinal Arthrodesis

Gurmit Singh, Sungsoo S. Lee, Timmy Fyrner, Mark T. McClendon, Karina K. Katchko, Andrew D. Schneider, Danielle S. Chun, Joseph A. Weiner, Ralph W. Cook, Justin T. Smith, Sameer Singh, Chawon Yun, Samuel I. Stupp, Erin L. Hsu, Wellington K. Hsu

Poster No. 392

WITHDRAWN

Poster No. 393

Magnesium Ion Enriched Bone Allograft for Large Bone Defect Management

Wenhao Wang, Hoi Man Wong, Paul K Chu, Frankie K.L. Leung, Kenneth M.C. Cheung, Kelvin Yeung

Poster No. 394

Mesenchymal Stem Cell Proliferation and Osteogenic Differentiation in 3D Printing Polycaprolactone-Hydroxyapatite(pcl/ha)scaffolds Combined with Marrow Clot

Fengyong Mao, Pengfei Zheng, Yue Lou, Kai Tang, Liming Wang, Qingqiang Yao

Poster No. 395

Plasma Enhanced Biocompatible and Photocatalytic Antibacterial Degradable Magnesium Alloy for Bone Fracture Fixation

Zhengjie Lin, Ying Zhao, Kenneth M.C. Cheung, Paul K. Chu, Kelvin Yeung, Frankie Leung

Poster No. 396

Efficacy of Wp9qy Peptide (w9) for Bone Formation in a Rat Delayed Union Model

Mikiya Sawa, Shigeyuki Wakitani, Nobuo Adachi, Yuriko Furuya, Mitsuo Ochi

Poster No. 397

Novel Biofunctional Material for Orthopedic Implants: Surface Chemistry, Corrosion and Biocompatibility Aspects

Luciana Daniele Trino, E.S. Bronze-Uhle, A. Ramachandran, Paulo Lisboa-Filho, Mathew Thoppi Mathew, Annie George

Poster No. 398

Poly(lactic-co-glycolic acid) Scaffold Coated with an Antioxidative Fullerene Derivative for Bone Tissue Engineering

Xinlin Yang, Guojun Ma, Yongfei Guo, Fuai Cui, Yazhou Li, Xiaodong Li, Quanjun Cui

Poster No. 399

Nell-1 Combined with Bone Marrow Aspirate Concentrate in a Polyelectrolyte Complex Based Construct Enhances Posterolateral Spinal Fusion in Rabbits

Ling Liu, Wing Moon Lam, Ming Wang, Mathanapriya Naidu, Felly Ng, Xia Fei Ren, Ting Kang, Chia Soo, James Goh, Hee Kit Wong

PS1 Biomaterials—Cartilage

Poster No. 400

Chondrocytes Produce Native-Like ECM Organization Using the MatriTek TissueSpec™ Cartilage Hydrogel Kit as a Scaffold for Cartilage Tissue Engineering When Nutrient Channels and CAGE Strategies are Employed

Wing-Sum A. Law, Krista M. Durney, Robert J. Nims, Gordana Vunjak-Novakovic, Clark T. Hung, Gerard A. Ateshian

Poster No. 401

Bone Bonding Double-Network Hydrogel for Cell-free Cartilage Regeneration: Influences of the Gel Thickness on the Regeneration Process In Vivo

Susumu Wada, Nobuto Kitamura, Takayuki Nonoyama, Ryuji Kiyama, Keiko Goto, Takayuki Kurokawa, Jian Ping Gong, Kazunori Yasuda

Poster No. 402

Bone Marrow-Mesenchymal Stem Cell Embedded Collagen-Based Chondroprogenitor Scaffold for the Treatment of Early Osteoarthritis in a Porcine Animal Model

Wo-Ran Tzeng, Shu-Wei Huang, Jui-Sheng Sun, Chih-Yu Chen, Chih-Hsiang Fang, Pei-I Tsai, Hsin-Hsin Shen, San-Yuan Chen, Feng Huei Lin

Poster No. 403

Acellular Cartilage Matrix Combined with Chitosan Cellulose Hydrogel for Cartilage Regeneration: Cell-Compatibility and Gene Expression Analysis

Chih-Hung Chang, Yu-Chun Chen, Ruo-Yu Chen, Yuan-Ming Hsu

Poster No. 404

Non-Destructive Vibrational Spectroscopic Assessment of Developing Chondrocyte-Seeded Hyaluronic Acid Constructs

Farzad Yousefi, Minwook Kim, Yusra Nahri, Robert L. Mauck, Nancy Pleshko

Poster No. 405

Arthritic Human Cartilage Molecular Engineering Using Biomimetic Proteoglycans Shows Infiltration Throughout the Cartilage Extracellular Matrix Ex Vivo

Evan Phillips, Nicholas Bertha, Brandon Shallop, Katsiaryna Prudnikova, Michele Marcolongo, Mary Mulcahey



2017 ANNUAL MEETING

PROGRAM BOOK

Sun-Wed, March 19-22, 2017 • San Diego Convention Center • San Diego, California

Plasma enhanced biocompatible and photocatalytic antibacterial degradable magnesium alloy for bone fracture fixation

Zhengjie Lin^{a,b}, Ying Zhao^c, Hoi Man Wong^{a,b}, Kenneth M C Cheung^a, Frankie Leung^{a,b}, Paul K. Chu^d, Kelvin W.K. Yeung^{a,b,*}

^aDepartment of Orthopaedics and Traumatology, The University of Hong Kong, Pokfulam, Hong Kong, China

^bShenzhen Key Laboratory for Innovative Technology in Orthopaedic Trauma, The University of Hong Kong Shenzhen Hospital, 1 Haiyuan 1st Road, Futian District, Shenzhen, China

^cCenter for Human Tissues and Organs Degeneration, Shenzhen Institutes of Advanced Technology, Chinese Academy of Sciences, Shenzhen 518055, China

^dDepartment of Physics and Materials Science, City University of Hong Kong, Tat Chee Avenue, Kowloon, Hong Kong, China

corresponding author Tel: +852 22554654; fax: +852 28174392

Email address: wkyeung@hku.hk

ABSTRACT INTRODUCTION: The use of magnesium alloy in orthopaedic procedures has attracted a lot of attentions in the field due to its degradability. However, rapid corrosion and subsequent hydrogen release *in vivo* conditions limit its clinical application. Thus, various methods e.g. alloying, coating, and heat treatment have been initiated in order to reinforce its corrosion property. In this study, plasma immersion ion implantation (PIII) technique has been developed to enhance the corrosion resistance and biocompatibility of WE43 magnesium alloy, while the antibacterial property can be triggered photocatalytically by UV light.

METHODS: The casted WE43 alloy was treated by titanium and oxygen dual plasma immersion ion implantation. The matrix was firstly subjected to titanium plasma ion implantation at 20kV for 2hrs and then followed by oxygen plasma ion implantation at 25kV for 3hrs. For surface characterizations of PIII-treated WE43 alloy, the atomic force microscope (AFM) and X-ray photoelectron spectroscopy (XPS) were conducted to investigate surface chemical states and morphology of the PIII-treated alloy, respectively. In order to systematically examine corrosion resistance of the untreated and PIII-treated alloys, immersion and electrochemical tests were conducted in the simulated body fluid (SBF) and DMEM culture medium at 37°C. The biocompatibility of PIII-treated WE43 alloy was cultured with mouse pre-osteoblastic (MC3T3-E1) cells and evaluated by using MTT, BrdU, ALP and RT-PCR assays. Moreover, the photocatalytic antibacterial property triggered by UV light illumination 1h was characterized by culturing with *S.aureus* and then assessed by live/dead staining. Also, the mechanism of photocatalytic antibacterial properties was investigated by measuring surface pH value and total reactive oxygen species (ROS) generated by the specimens during bacterial culture.

RESULTS SECTION: The XPS and AFM results indicated that the surface of treated WE43 magnesium alloy appeared a semi-dense protective layer with the thickness of about 120 nm created by titanium and oxygen dual implantation. The protective layer was mainly comprised TiO₂ and MgO. The electrochemical tests in SBF proved that the PIII-treated WE43 alloy exhibited excellent performance of corrosion resistance as compared with the untreated control. The direct cell assay proposed that the cells were flattened and spread on PIII treated sample surface, while cultured with the pre-osteoblasts. A large amount of F-actins were observed on the surface of PIII-treated WE43 alloy. When the cells cultured with extracts of PIII-treated WE43 alloy, the result of MTT, BrdU and ALP assays suggested that the cell viability and proliferation were much higher as compared with the untreated control. Furthermore, the osteogenic expressions including ALP, Type I Col I, Runx2 and OPN of pre-osteoblasts were significantly up-regulated as well. These results indicated that the cyto-compatibility of WE43 alloys can be significantly improved by titanium and oxygen dual PIII treatment. In addition, the *S.aureus* were 99.98% killed on the surface of PIII-treated magnesium alloy due to the release of ROS, indicating that the photocatalytic antibacterial property of TiO₂ layer on PIII-treated WE43 alloy can be triggered by UV light illumination.

DISCUSSION: The semi-dense TiO₂ layer established by Ti and O dual plasma immersion ion implantation can apparently enhance the corrosion resistance of WE43 alloy. It is believed that the semi-dense layer can effectively suppress the rapid corrosion of magnesium alloy, while it may also allow the release of Mg ions from the substrate. The cyto-compatibility can be enhanced due to the suppression of excess Mg ion released and less hydrogen gas generation. Our previous study proved that the concentration of magnesium ions at 50-200 ppm can effectively promote the bone cell proliferation and up-regulation of osteogenic genes *in vitro* and new bone formation under *in vivo* [1]. Regarding to the photocatalytic antibacterial property, we believe that the mechanism is highly because of the generation of ROS e.g. ^{*}O₂, ^{*}OH on TiO₂ layer after stimulated by UV light. These ROS elements are able to destroy the cell membrane of *S.aureus* and then bacteria killed.

SIGNIFICANCE: The corrosion resistance and cyto-biocompatibility of WE43 magnesium alloys can be significantly enhanced by Ti and O dual plasma immersion ion implantation. This specially treated alloy also exhibits photo-catalytic antibacterial property when simulated by UV light. Hence, it is believed that the PIII-treated WE43 magnesium alloy may consider applying for orthopaedic bone fracture fixation when the *in vivo* pre-clinical analyses are systematically investigated.

REFERENCES: [1] H.M. Wong. *Biomaterials*. 2013;34:7016-7032.

IMAGES AND TABLES:

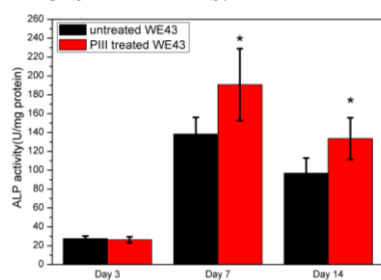


Fig.1 Osteoblasts differentiation evaluated by ALP assay of MC3T3-E1 pre-osteoblasts cultured with the extracts of untreated WE43 and PIII-treated WE43 all incubation in DMEM at 37°C for 3,7 and 14 days. *denotes the significant difference between PIII-treated WE43 alloy and untreated WE43 alloy (p<0.05)

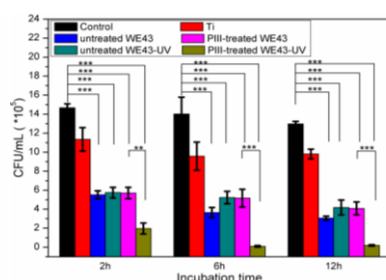


Fig 2. The effect of TiO₂ coating illuminated by UV light on the growth of *S.aureus* bacterial seeded on the surface of WE43 based alloys. The control was *S.aureus* suspension (CFUs 10⁶/ml) without any Ti or magnesium alloys. * denotes significant difference between PIII-treated WE43-UV and PIII-treated WE43 group (p<0.05); ** (p<0.01); *** p<0.001.

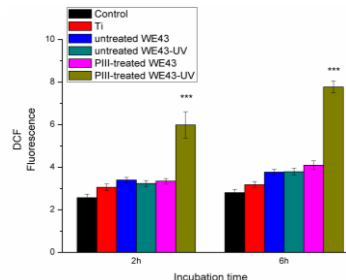


Fig 3. The effect of TiO₂ coating illuminated by UV light on *S.aureus* cellular total ROS probed with 2,7-dichlorofluorescein diacetate (DCFH-DA) detected *S.aureus* bacterial seeded on the surface of WE43 based alloys. The control was *S.aureus* suspension (CFUs 10⁶/ml) without any Ti or magnesium alloys. * denotes significant difference between PIII-treated WE43-UV and PIII-treated WE43 group (p<0.05); ** (p<0.01); *** p<0.001.